Vibrational dynamics of aniline (N$_2$)$_1$ clusters in their first excited singlet state

M. F. Hineman, S. K. Kim, E. R. Bernstein, and D. F. Kelley

Vibrational dynamics of aniline (N$_2$)$_1$ clusters in their first excited singlet state

M. F. Hineman, S. K. Kim,[a] E. R. Bernstein,[b] and D. F. Kelley[b]
Colorado State University, Chemistry Department, Fort Collins, Colorado 80523

The first excited singlet state S^1 vibrational dynamics of aniline(N$_2$)$_1$ clusters are studied and compared to previous results on aniline(CH$_4$)$_1$ and aniline(Ar)$_1$. Intramolecular vibrational energy redistribution (IVR) and vibrational predissociation (VP) rates fall between the two extremes of the CH$_4$ (fast IVR, slow VP) and Ar (slow IVR, fast VP) cluster results as is predicted by a serial IVR/VP model using Fermi's golden rule to describe IVR processes and a restricted Rice–Ramsperger–Kassel–Marcus (RRKM) theory to describe unimolecular VP rates. The density of states is the most important factor determining the rates. Two product states, 0^0 and $10b^1$, of bare aniline and one intermediate state $\overline{0^0}$ in the overall IVR/VP process are observed and time resolved measurements are obtained for the 0^0_0 and $\overline{0^0_0}$ transitions. The results are modeled with the serial mechanism described above.

I. INTRODUCTION

The vibrational dynamics of van der Waals (vdW) clusters have recently attracted considerable experimental and theoretical attention. The most extensively studied vdW clusters consist of a chromophore molecule and one or more solvent molecules. The cluster is excited by absorption of a photon ($S_1 \leftarrow S_0$) to a chromophore vibronic state which can then relax by three different pathways: (1) fluorescence or radiationless processes (intersystem crossing or internal conversion); (2) intracluster vibrational redistribution of the excess chromophore vibrational energy to the van der Waals modes (IVR); and (3) vibrational predissociation (VP) if the chromophore vibrational energy is greater than the cluster binding energy.

The overall IVR/VP process has been suggested to occur by two different mechanisms. The first is a parallel mechanism in which the vibrationally excited chromophore undergoes IVR and VP in uncoupled steps: that is, the cluster vibronic chromophore level accessed can relax to other cluster chromophore plus vdW mode states of the cluster and/or it can couple directly to the continuum states which correspond to two bare molecules (VP). The vast majority of vdW cluster spectroscopic and dynamical results have been interpreted in terms of a parallel mechanism.[1–4] The second mechanism for the IVR/VP process is a serial mechanism, in which IVR and VP are inextricably coupled. In the serial mechanism IVR from the chromophore modes to the vdW modes must precede VP. Cluster VP, generating bare molecules, occurs only if IVR has placed enough energy in the vdW modes to break the intermolecular bond between the solvent and the chromophore. These processes have been modeled[5,6] using Fermi's golden rule[7] and a restricted Rice–Ramsperger–Kassel–Marcus (RRKM) treatment of unimolecular rate constants[8] which takes into account only vdW modes.

In a recent paper from this laboratory[5] we have concluded that the serial mechanism is the more appropriate of the two for the aniline(CH$_4$)$_1$ and aniline(Ar)$_1$ clusters. We have also analyzed the dynamical results[9] for tetrazine (Ar)$_1$ within the framework of a serial model.[6] These clusters have spacings between the chromophore vibrational energy levels which are small compared to the cluster binding energy, and a relatively high density of vdW mode states near the cluster binding energy. We have suggested that the above are necessary and sufficient conditions for the serial model to be operative,[5,6] and thus we conclude that for systems such as benzene, tetrazine, and aniline, clustered with argon, nitrogen, methane, water, ammonia, etc. and aromatic dimers, a serial mechanism is most appropriate.

The experimental demonstration that a serial mechanism (first chromophore to vdW mode IVR and then VP) is indeed correct and can come from two sources: (1) fitting the observed rise and fall times of various bare molecule and cluster features with a minimum of arbitrary parameters [e.g., only one parameter for both aniline(Ar)$_1$ and aniline(CH$_4$)$_1$ clusters[5]]; and (2) direct observation of the kinetics of intermediate cluster states for which some or all of the IVR, but no VP has occurred. The first type of evidence for the serial mechanism has been offered in the recent literature.[5,6] In this paper we present both types of evidence for an overall serial IVR/VP dynamic mechanism in vdW clusters for which the density of vdW states is high. The specific system for which these results have been obtained is aniline(N$_2$)$_1$. This system is of particular interest because of the comparison to the previously studied aniline(Ar)$_1$ and aniline(CH$_4$)$_1$ clusters.

II. EXPERIMENT

The experimental apparatus consists of a cw molecular jet with a picosecond laser/time correlated single photon counting detection system which has been described in detail previously.[5] The carrier gas mixture is varied between 0.2% and 1.5% nitrogen in helium at a total pressure of 3–4 atm.

Aniline is introduced into the carrier gas at its room temperature vapor pressure (< 1 Torr). The fluorescence is dispersed using a 2400 grooves/mm grating in a 1.0 m monochromator which, used in first order, results in a total instrument time response function of 150 ps FWHM. This system is also used to take dispersed emission spectra as described previously.[5] Mass selected excitation spectra are obtained using a time of flight photoionization mass spectrometer which has also been detailed in earlier papers.[10]

III. RESULTS

A. Mass resolved excitation spectra

The mass resolved spectrum of the aniline monomer has been published.[5] The 0_0^0 transition of bare aniline appears at 34 032 cm^{-1} and strong transitions are assigned to $6a_0^1$ (0_0^0 + 493 cm^{-1}), 15_0^2 (0_0^0 + 718 cm^{-1}), I_0^2 (0_0^0 + 749 cm^{-1}), and 1_0^1 (803 cm^{-1}). The mass resolved spectrum of aniline $(N_2)_1$ shows the origin and its vibronic peaks are shifted approximately 130 cm^{-1} to the red of the bare aniline 0_0^0 transition (see Fig. 1). In addition, peaks appear at 55 and 68 cm^{-1} higher energy than the cluster origin $\overline{0_0^0}$, and are assigned to $\overline{0_0^0}$ plus excitations of the van der Waals modes. (The notational convention of using a bar across the top of all transitions of the cluster species is adopted here.) These bands do not appear in the bare aniline spectrum and cannot be assigned as internal modes of the aniline molecule. A possible assignment to hot bands can also be ruled out because of the low temperature of the clusters in the jet. Similar peaks red shifted from the $\overline{0_0^0}$ transition are observed in the dispersed emission spectrum after $\overline{0^0}$ excitation. In the vicinity of the S_1 origin, the mass resolved excitation spectrum of aniline$(N_2)_2$ shows only a broad feature (width ~300 cm^{-1}) shifted to the red by an additional 130 cm^{-1}.
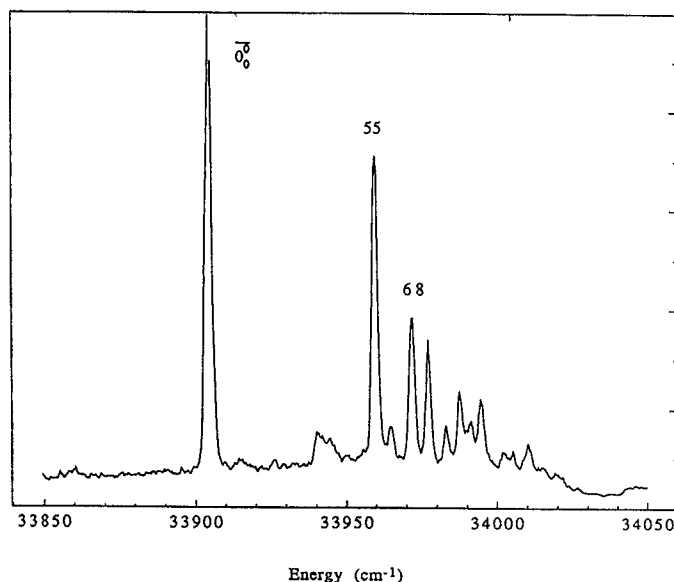

FIG. 1. Time-of-flight mass selected excitation spectrum of aniline$(N_2)_1$, in the origin region showing the van der Waals mode excitations at 55 and 68 cm^{-1}.
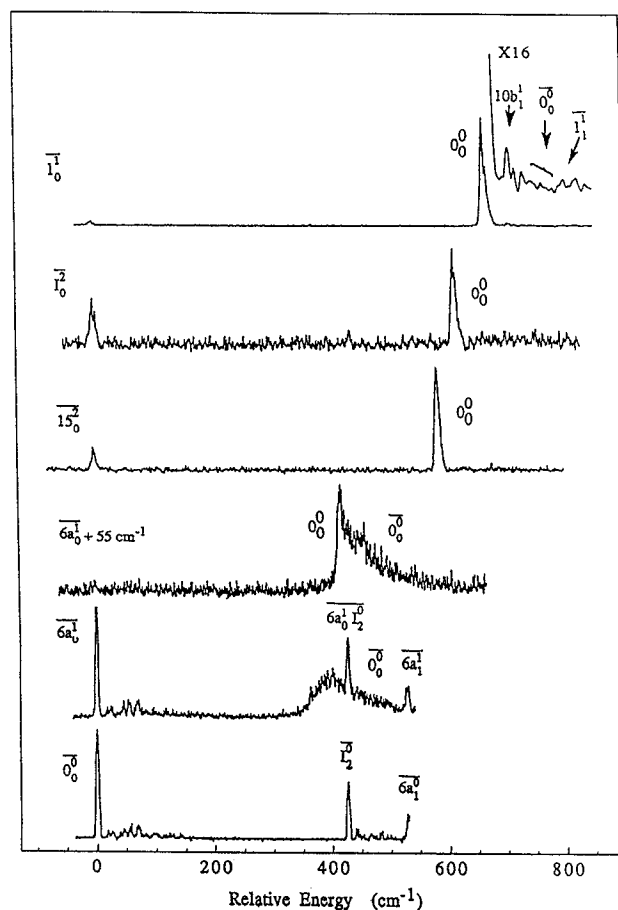

FIG. 2. Dispersed emission spectra of aniline$(N_2)_1$ clusters following excitation to several vibrational states of S_1. Relative energy is the shift, in wave numbers, from the excited transition. The top spectrum ($\overline{1_0^1}$ excitation) shows an inset trace for an expanded scale about the 0_0^0 intense feature. $10b_1^1$, $\overline{0_0^0}$, and $\overline{1_1^1}$ emission can be observed. Note that the relaxed cluster emission from $\overline{0_0^0}$ (following IVR) is broad as expected (compare to $\overline{6a_0^1}$ + 55 cm^{-1} and $\overline{6a_0^1}$ excitation).

B. Dispersed emission spectra and lifetime measurements

The dispersed emission (DE) spectra of the aniline$(N_2)_1$ cluster following excitation to several vibrational states in S_1 are shown in Fig. 2. The emission kinetic curves for several transitions following $\overline{1^1}$ excitation are shown in Fig. 3. The time dependence information is collected in Table I.

Following $\overline{0^0}$ excitation, strong emission from the pumped state is observed. The 7.4 $\pm$ 0.5 ns lifetime of this emission matches the 7.8 ns bare aniline excited state lifetime within experimental uncertainty, showing that neither the electronic transition moment nor the modes of radiationless decay which control the emission lifetime are strongly perturbed by the presence of the N_2 molecule.

Excitation to $\overline{6a^1}$ yields, in addition to pumped state transitions, a broad emission band between 370 and 490 cm^{-1} red shifted from the excitation. This feature is assigned to emission from the hot cluster $\overline{0^0}$ state (i.e., $\overline{0^0}$ plus ca.
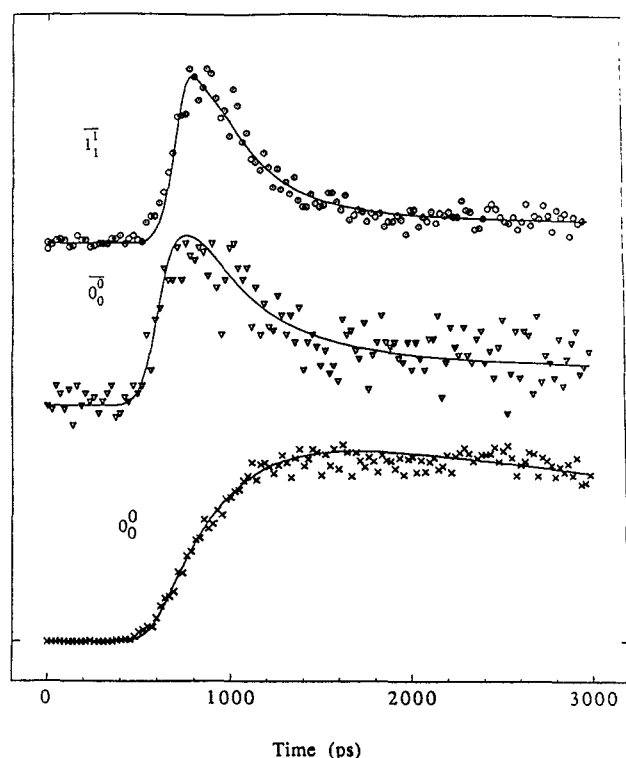
FIG. 3. Decay curves and fits for several emission bands following $\overline{1^1}$ excitation of the aniline$(N_2)_1$ cluster.

Since the cold cluster spectrum is red shifted 130 cm^{-1} from the bare aniline spectrum and since substantial vdW mode activity is present in the $S_1 \leftarrow S_0$ cold cluster spectrum (see Fig. 1), we conclude that the S_1 binding energy is greater than the S_0 binding energy and that the equilibrium position for S_1 surface is shifted to smaller aniline–nitrogen separations. These two differences can have a substantial effect on the emission spectrum of the aniline$(N_2)_1$ cluster if a large amount of energy is present in the vdW modes. This energy is distributed in general amongst the five cluster vdW modes. Emission occurs from regions of the S_1 vdW potential surface corresponding to ca. 500 cm^{-1} of excess vibrational energy in the vdW modes and thus large aniline–nitrogen displacements. The observed emission occurs vertically to the corresponding regions of the S_0 potential surface. Because the S_0 surface is shallower than the S_1 surface, the aniline–nitrogen separation is larger in S_0 than in S_1, and the density of vdW states is large at 500 cm^{-1} of excess vibrational energy, the resulting hot emission is blue shifted relative to the cold $\overline{0_0^0}$ transition and quite broad. As shown in Fig. 2, the observed shift is ca. 100 cm^{-1} and its width is ca. 100 cm^{-1} FWHM.

Following $\overline{6a^1}$ excitation, no 0_0^0 peak, which would be populated by VP of the cluster, is observed. The observation of a broad $\overline{0_0^0}$ emission after $\overline{6a^1}$ excitation is analogous to what is observed for aniline$(CH_4)_1$ clusters.[5] Emission from the aniline(N_2) pumped state decays in $\sim$3 ns; the broad $\overline{0_0^0}$ emission band exhibits a $\sim$3 ns risetime and decays with the aniline S_1 lifetime.

Excitation to ($\overline{6a^1}$ + quanta in the vdW modes) generates spectra which contain the broad envelope previously assigned to the $\overline{0_0^0}$ + vdW modes. Emission from the bare aniline molecule (0_0^0) is also observed upon excitation of $\overline{6a_0^1}$ + 55 cm^{-1}. The total integrated intensity of the $\overline{0_0^0}$ emission is about 6.8 times that of the 0_0^0 emission. The risetime of the $\overline{0_0^0}$ envelope emission is approximately 0.4 ns. Kinetics of the 0_0^0 band could not be obtained due to overlap with the broad $\overline{0_0^0}$ band. The decay time of the broad $\overline{0_0^0}$ emission is 7.2 $\pm$ 0.5 ns.

Additionally, the weaker $\overline{6a^1}$ + 68 cm^{-1} state is also excited, but the emission kinetics of this feature are not consistent with the observed $\overline{0_0^0}$ and 0_0^0 emission intensity ratio. The $\overline{6a_0^1}$ + 68 cm^{-1} transition has very low intensity, about one-third that of the $\overline{6a_0^1}$ + 55 cm^{-1} transition. The cause of this internal inconsistency is most likely interference from higher order van der Waals clusters which is unavoidable on such a weak transition.

Excitations of the cluster to $\overline{1^1}$, $\overline{I^2}$, and $\overline{15^2}$ show results which are quite similar to each other. Emission from the state pumped is very weak, as is the $\overline{0_0^0}$ emission. The dominant peak observed upon these excitations is the bare molecule 0_0^0 transition. In spite of the weakness of these features, in the case of $\overline{1^1}$ excitation $\overline{1_1^1}$ and $\overline{0_0^0}$ emission kinetics can be obtained and are shown in Fig. 3. The decay of the $\overline{1^1}$ state occurs in $\sim$0.3 ns. The $\overline{0_0^0}$ transition follows

500 cm^{-1} in the vdW modes) terminating in the $\overline{0^0}$ + ca. 500 cm^{-1} in the vdW modes of the ground state. This $\overline{0^0}$ plus ca. 500 cm^{-1} in the vdW modes is generated by IVR from the $\overline{6a^1}$ state. The broad emission envelope associated with this hot cluster transition has a substantial blue shift from the expected 490 cm^{-1} interval based on the $\overline{6a_0^1}$ and $\overline{0_0^0}$ transition energy difference. The blue shift and width are due to the differences in the excited and ground state vdW potential surfaces and the Franck–Condon factors associated with transitions between these two electronic surfaces.

TABLE I. Observed rise and decay times (ns) of fluorescence emissions of aniline $(N_2)_1$ clusters excited to various vibrational states.

Cluster state excited	Transition observed	Rise time	Decay time
$\overline{0^0}$	$\overline{0_0^0}$	0	7.4 $\pm$ 0.5
$\overline{6a^1}$	$\overline{6a_0^1}$	0	2.9 $\pm$ 0.2
$\overline{6a^1}$	$\overline{0_0^0}$	3.25 $\pm$ 0.3	7.4 $\pm$ 0.5
$\overline{6a^1}$ + 55 cm^{-1}	$\overline{0_0^0}$	0.4 $\pm$ 0.1	7.2 $\pm$ 0.5
$\overline{15^2}$	0_0^0	0.3 $\pm$ 0.1	8.2 $\pm$ 0.5
$\overline{I^2}$	0_0^0	0.3 $\pm$ 0.1	7.2 $\pm$ 0.5
$\overline{1^1}$	$\overline{1_1^1}$	0	0.3 $\pm$ 0.05
$\overline{1^1}$	$\overline{0_0^0}$	0	0.35 $\pm$ 0.1
$\overline{1^1}$	0_0^0	0.37 $\pm$ 0.05	8.0 $\pm$ 0.5

these kinetics (instrument limited rise, followed by a 0.3 ns decay) to within experimental error. The 0_0^0 transition of the bare molecule rises in 0.3 ns, corroborating the cluster kinetics. The dispersed emission spectrum following $\overline{1^1}$ excitation shows a small peak due to $10b_1^1$ emission of the bare aniline. There is, however, a significant broad background beneath this peak. Thus, the $10b^1$ kinetics are contaminated, presumably from higher order cluster emission. The $\overline{10b_1^1}$ emission is expected to be both broad and weak, and was not observed in the DE spectrum.

$$[A = \overline{6a^1} + 55 \text{ cm}^{-1}, \overline{1^1}, \overline{I^2} \text{ or } \overline{15^2}, B = \overline{0^0}, C = 0^0]$$
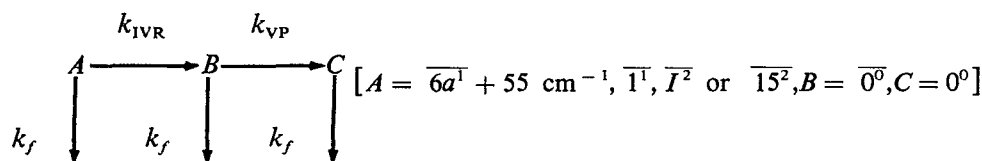
in which k_{IVR} and k_{VP} are the IVR and VP rates, respectively and k_f is the fluorescence rate (1/7.8 ns). This mechanism ignores intermediate states populated by IVR (i.e., states with vibrational excitation in both chromophore and vdW modes). As discussed above, these intermediate states are short lived, and do not significantly alter the kinetics. At $t = 0$ we have $[A] = [A]_0$, $[B] = [C] = 0$, and the concentrations as a function of time are given by

$$[A] = [A]_0 e^{-(k_{IVR} + k_f)t},$$

$$[B] = \frac{k_{IVR}[A]_0}{(k_{VP} - k_{IVR})} e^{-k_f t} \{ e^{-k_{IVR}t} - e^{-k_{VP}t} \},$$

$$[C] = [A]_0 e^{-k_f t} \left\{ 1 + \frac{1}{k_{IVR} - k_{VP}} \right.$$

$$\left. \times [k_{VP} e^{-k_{IVR}t} - k_{IVR} e^{-k_{VP}t}] \right\}. \quad (1)$$

The spectra and kinetics obtained following $\overline{6a^1} + 55$ cm^{-1} excitation can be interpreted in terms of this model. Specifically, the kinetic results are internally consistent with the relative intensities of the $\overline{0_0^0}$ and 0_0^0 emissions within the framework of a serial IVR/VP mechanism. The ratio of cluster to bare molecule origin intensities (~ 6.8) is given by the ratio of the time integrals of the expressions for $[B]$ and $[C]$ in Eq. (1). Taking these integrals and simplifying, one finds this is just the ratio of the fluorescence and vibrational predissociation decay rates, k_f/k_{VP}. This ratio along with a 7.8 ns emission lifetime (k_f^{-1}) implies that k_{VP} is (53 ns)$^{-1}$. The observed lifetime of the $\overline{0^0}$ cluster state is determined by both the usual decay paths and by VP, $k_{obs}^{-1} = (k_f + k_{VP})^{-1}$. Taking $k_f^{-1} = 7.8$ ns and and $k_{VP}^{-1} = 53$ ns, the observed lifetime is calculated to be 6.8 ns in reasonable agreement with the observed 7.2 $\pm$ 0.5 ns.

The spectra and kinetics obtained following $\overline{15^2}$, $\overline{I^2}$, and $\overline{1^1}$ excitation can also be analyzed in terms of a serial mechanism. The relative rates of initial state IVR (k_{IVR}) and intermediate state (e.g., $\overline{0^0}$)VP(k_{VP}) are crucial to this analysis and simplification of Eq. (1).

IV. DISCUSSION

The above data can be explained by a serial IVR/VP mechanism in which energy is transferred from the chromophore vibrational modes to the vdW modes prior to VP. Once the amount of energy in vdW modes exceeds the dissociation energy of the complex, VP can proceed or further energy transfer from chromophore modes may occur.

A simplified three state version of this mechanism can be modeled as

The IVR rate can be modeled using the Fermi's golden rule approximation in which transition probabilities depend on coupling between initial and final states, and the density of final states. There are two major results of this model: a general "energy gap law" for the IVR process under which the rate of IVR decreases as greater numbers of quanta are exchanged between the initial and final states; and the rate of IVR increases with the density of vdW receiving (final) states, $N(E)$. Similar ideas have been suggested by Ewing[11] and by Weber and Rice.[12] The form of the energy gap term depends on assumptions made about the details of the potential surface. For lack of a better alternative, we have used a model describing energy transfer in low temperature matrices. The result is a term proportional to $\exp[-(E_{ij}/h\nu_{max})^{1/2}]$ in which E_{ij} is the energy transferred in the IVR process upon going from the jth to the ith chromophore energy level and $h\nu_{max}$ is the energy of one quanta in the highest frequency vdW mode. The ratio $E_{ij}/h\nu_{max}$ is roughly proporational to the number of quanta deposited into the vdW modes by the IVR transition. (If ν_{max} corresponded to the only receiving mode, then the above statement would be exactly correct. However, other vdW modes must also be involved for a golden rule expression to be valid.) The final rate constant for IVR is then taken to be

$$k_{IVR} = (A/\nu_i) \exp[-(E_{ij}/h\nu_{max})^{1/2}]N(E_i). \quad (2)$$

ν_i in Eq. (2) refers to the frequency of the ith chromophore vibration (populated by the IVR transition), and the proportionality to $1/\nu_i$ is purely phenomenological. This proportionality reflects the expectation that low frequency chromophore modes will couple most efficiently to the (low frequency) vdW modes. Fermi's golden rule expression has two important consequences. First, it predicts that IVR will be much faster in clusters with more vdW degrees of vibrational freedom, and hence higher densities of states. Second, it predicts that the slowest IVR transitions will be from the initially excited state, as subsequent IVR transitions result in more energy in the vdW modes, and hence a higher density of receiving states. Thus, depopulation of the initially excited

state is expected to be the rate limiting IVR step.

The VP rate is calculated by a restricted (to vdW modes) RRKM theory. By assuming a "tight binding" model for the cluster transition state the resulting expression for the VP rate constant is[8]

$$k_{VP} = \frac{1}{h} \left[\Sigma P_v (E - E_0)/N(E) \right]$$

in which $\Sigma P_v (E - E_0)$ is the sum of vdW states above the dissociation threshold, $N(E)$ is the density of vdW states, E is the amount of vibrational energy in the vdW modes, and E_0 is binding energy. In the Marcus–Rice approximation, these are given by

$$\Sigma P_v (E - E_0) = (E - E_0)^{S-1}/(S-1)!\Pi' h v_i$$

and

$$N(E) = E^{S-1}/(S-1)!\Pi h v_i$$

in which S is the number of vdW vibrational modes, the product is over the vdW mode energies and the prime excludes the reaction coordinate. Using the above approximations, we get

$$k_{VP} = \left(\frac{E - E_0}{E} \right)^{S-1} v \qquad (3)$$

in which v is the frequency of the vibrational mode corresponding to the reaction coordinate. For a given cluster, k_{VP} always increases as $(E - E_0)$ increases; however, at a given $(E - E_0)$, the cluster with the fewer vdW vibrational modes and hence the smaller density of vdW states will have the larger k_{VP}.

The above model makes qualitative and semiquantitative predictions about the IVR and VP rates in different clusters. Of particular relevance is the comparison of the IVR and VP rates for the clusters aniline$(CH_4)_1$, aniline$(N_2)_1$, and aniline$(Ar)_1$: aniline$(Ar)_1$ has only the three vdW modes; aniline$(CH_4)_1$ has six vdW modes; and aniline$(N_2)_1$ has five vdW modes. As a result, the sums and densities of vdW states used in the calculations of k_{IVR} and k_{VP} are quite different in these three clusters. Since the chromophore in these clusters remains the same, however, initial excitation to the same energy in each cluster is possible. Furthermore, we expect that the extent of chromophore–solvent interaction will not be vastly different in these cases; that is, the A term in Eq. (1) will be of the same order of magnitude for each cluster. The IVR rates for the N_2 cluster are expected to fall below those of the CH_4 cluster but above those of the Ar cluster as the density of vdW states at a given cluster energy increases with the number of vdW vibrational modes. Table II shows the observed trend: τ_{IVR} (Ar) $> \tau_{IVR}$ $(N_2) > \tau_{IVR}$ (CH_4). The sharp decrease in decay time of the pumped state for $\overline{6a^1} + 55$ cm^{-1} compared to $\overline{6a^1}$ can be explained by the increase in vdW state density as the number of quanta in the vdW modes increases.

The VP rates are predicted to order in the opposite manner, as they depend inversely on the density of states. The energy in the vdW modes accesses phase space in a statistical manner according to RRKM theory and the greater the number of modes, the smaller is the probability that the energy is in the reaction coordinate. The calculated RRKM VP

TABLE II. Comparison of IVR lifetimes for aniline (X_1) clusters with $X = Ar, N_2$, or CH_4. Times are calculated by removing the S_1 lifetime from the experimental decay times. Measured times (ns) are accurate to $+15\%$ or $+0.1$ ns whichever is greater.

Cluster state excited	Vibrational energy (cm^{-1})	τ_{IVR} X = Ar [a]	τ_{IVR} X = N$_2$	τ_{IVR} X = CH$_4$ [a]
$\overline{6a_0^1}$	493	11	4.5	<0.1
$\overline{6a_0^1} + 55$ cm^{-1}	548		0.4	
$\overline{15_0^2}$	718	1.8	0.3	<0.1
$\overline{I_0^2}$	749		0.3	
$\overline{1_0^1}$	803	4.0	0.36	<0.1

[a] Calculated from Ref. 5 results.

rate is sensitive to the assumed binding energy E_0. The spectra can be used to estimate the aniline(N_2) binding energy. The absence of 0_0^0 emission following $\overline{6a^1}$ excitation indicates that if 493 cm^{-1} of vibrational energy is placed in the vdW modes, dissociation does not occur or is slow compared to the 7.8 ns emission lifetime. Also, the presence of 0_0^0 emission following $\overline{6a^1} + 55$ cm^{-1} excitation indicates that the value at E_0 must be less than 548 cm^{-1}. Thus, we infer that the value at E_0 cannot be much above or below 500 cm^{-1}.

The binding energy can be accurately estimated (assuming that RRKM theory accurately describes the dissociation process) by fitting an E_0 which predicts the observed VP rate for $\overline{6a^1} + 55$ cm^{-1} excitation. This VP$[\sim (53$ ns$)^{-1}]$ rate is determined from the integrated intensities of the $\overline{0_0^0}$ and 0_0^0 emission bands as described above. Because of the partial overlap of the two emission bands, decay measurements of the bare aniline emission are not conclusive, as they are dominated by the $\overline{0_0^0}$ emission. Nonetheless, since the fluorescence lifetimes are known, the integrated intensities provide the necessary information. From this analysis, a value of 515 cm^{-1} is obtained. This is fairly close to the 450 and 480 cm^{-1} values obtained for argon and CH_4 clusters, respectively, as one would expect. Equations (2) and (3) can be used to make estimates of the relative magnitudes of the IVR and VP rates.

Excitation of the $\overline{15^2}$, $\overline{I^2}$, and $\overline{1^1}$ levels results in about 203, 234, and 288 cm^{-1} of energy in excess of the cluster binding energy. If the aniline $(N_2)_1$ cluster has more than about 200 cm^{-1} of excess vibrational energy (i.e., $E > E_0 + 200$ cm^{-1}), the VP rate for $\overline{0^0}$ given by Eq. (3) is larger than $\sim (100$ ps$)^{-1}$. This is considerably faster than the IVR rate of the initially accessed state. Therefore simplifying Eq. (1), we take $k_{VP} \gg k_{IVR}$ and for times longer than the instrument response function, we take $k_{VP} t \gg 1$. Under these circumstances, we get

$$[B] \sim \frac{k_{IVR}}{k_{VP}} [A]_0 e^{-(k_{IVR} + k_f)t}$$

and

$$[C] \sim [A]_0 e^{-k_f t} \{1 - e^{-k_{IVR}t}\}.$$

TABLE III. Comparison of experimentally observed and (calculated) VP lifetimes (ns) for aniline (X_1) clusters, where X = Ar, N_2, or CH_4. Binding energies for the clusters are 450, 515, and 480 cm^{-1}, respectively. All energies in cm^{-1}.

Cluster state excited	Vibrational energy	Transition observed	X = Ar[b] excess energy	τ_{VP}	X = N_2 excess energy	τ_{VP}	X = CH_4[b] excess energy	τ_{VP}
$\overline{6a^1}$	493	0_0^0	43	<0.1(0.08)			13	150[a] (40,000)
$\overline{6a^1}$ + 55 cm^{-1}	548	0_0^0			33	53[a](60)		
$\overline{6a^1}$ + 68 cm^{-1}	561	0_0^0			46	19[a](16)		
$\overline{15^2}$	718	0_0^0	268	<0.1(0.004)	203		238	0.24 (.18)
$\overline{1^2}$	749	0_0^0	299		234			
$\overline{1^1}$	803	0_0^0	353	<0.1(0.003)	288	<0.1(0.04)		

[a] Determined by integrated peak ratios because overlapping bands perturb the decay curves for these states.
[b] From Ref. 5.

Therefore, in such cases the observed $\overline{0_0^0}$ kinetics [B] are predicted simply to follow the kinetics of the accessed state. Also, the risetime of the 0_0^0 emission (the [C] kinetics) is predicted to match the decay of the $\overline{1^1}$ state and $\overline{0^0}$ states. This is exactly the behavior that is observed and is shown in Fig. 3 for the case of $\overline{1^1}$ excitation.

This result is in sharp contrast to what is predicted by a parallel mechanism. The parallel mechanism predicts that similar kinetics should be observed for both $\overline{0_0^0}$ and 0_0^0 emissions: Both should rise with the decay at the $\overline{1^1}$ state, and decay with the 7.8 ns emission lifetime.

A quite different situation is obtained for aniline$(CH_4)_1$. In this case, the VP rate of the $\overline{0^0}$ state is much smaller than the IVR rate of the accessed state and consequently the observed decay of the $\overline{0^0}$ state is dominated by its own dissociation kinetics.

In the case of $\overline{1^1}$ excitation, some $10b_1^1$ emission is also observed, indicating that the above three state model is only approximately correct. The model can easily be generalized to include the $\overline{10b^1}$ and $10b^1$ states. If the $\overline{10b^1} \rightarrow \overline{0^0}$ IVR rate is taken to be fast [as predicted by Eq. (2)], then little population ends up in $10b^1$, in agreement with the observed results.

A summary of both experimental and calculated results for aniline clusters studied to date is given in Table III.

The most remarkable and central observation of these experiments is the direct characterization of the emission kinetic curves for the $\overline{1_1^1}$, $\overline{0_0^0}$, and 0_0^0 transitions and the observation of the $10b_1^1$ transition following excitation at $\overline{1^1}$ of the aniline$(N_2)_1$ cluster. The pumped state, an intermediate state populated by IVR, and two bare molecule product states populated by the IVR/VP process are observed. These data are consistent with, and therefore provide strong evidence in support of, the serial IVR/VP mechanism applied to clusters containing a polyatomic chromophore. A parallel mechanism simply cannot explain the observed results.

V. CONCLUSIONS

The general conclusions which we derive from these experiments can be summarized as follows:

(1) the experimental results follow the predictions of a serial IVR/VP mechanism in which IVR is described by Fermi's golden rule and VP is described by a restricted RRKM model;

(2) aniline$(N_2)_1$ clusters undergo IVR and VP dynamics which are intermediate with respect to the aniline$(CH_4)_1$ and aniline$(Ar)_1$ clusters observed in previous studies; and

(3) the most important factor in the determination of IVR and VP rates is the density of vdW states at a given excess vibrational energy.

We have demonstrated these general conclusions by two analytical approaches: all the data are fit with the serial IVR/VP model using one parameter in the same manner as has been accomplished for other aniline and tetrazine complexes; and the intermediate cluster state $\overline{0^0}$ ($\overline{1^1} \rightarrow \overline{0^0} \rightarrow 0^0$) dynamics have been measured and the rise and fall times are consistent with those of the nascent and final state dynamics.

ACKNOWLEDGMENT

[1] (a) K. W. Butz, D. L. Catlett, Jr., G. E. Ewing, D. Krajinovich, and C. S. Parmenter, J. Phys. Chem. **90**, 3533 (1986); (b) B. A. Jacobson, S. Humphrey, and S. A. Rice, J. Chem. Phys. **89**, 5624 (1988); (c) H.-K. O, C. S. Parmenter, and M. C. Su, Ber. Bunsenges, Phys. Chem. **92**, 253 (1988).

[2] T. A. Stephenson and S. A. Rice, J. Chem. Phys. **81**, 1083 (1984).

[3] B. A. Jacobson, S. Humphrey, and S. A. Rice, J. Chem. Phys. **89**, 5624 (1988); T. A. Stephenson and S. A. Rice, *ibid.* **81**, 1083 (1984).

[4] J. C. Alfano, S. J. Martinez III, and D. H. Levy, J. Chem. Phys. **91**, 7302 (1980); D. V. Brumbaugh, J. E. Kenney, and D. H. Levy, *ibid.* **78**, 3415 (1983).

[5] M. R. Nimlos, M. A. Young, E. R. Bernstein, and D. F. Kelley, J. Chem. Phys. **91**, 5268 (1989).

[6] D. F. Kelley and E. R. Bernstein, J. Phys. Chem. **90**, 5164 (1986).

[7] (a) P. Avouris, W. M. Gelbart, and M. A. El-Sayed, Chem. Rev. **77**, 793 (1977); (b) S. Mukamel, J. Phys. Chem. **89**, 1077 (1985); (c) S. Muka-

mel and J. Jortner, *Excited States*, edited by E. C. Lim (Academic, New York, 1977), Vol. III, p. 57.

[8] (a) D. J. Robinson and K. A. Holbrook, *Unimolecular Reactions* (Wiley, New York, 1972); (b) J. I. Steinfeld, J. S. Francisco, and W. L. Hase, *Chemical Kinetics and Dynamics* (Prentice Hall, New York, 1989); (c) R. D. Levine and R. B. Bernstein, *Molecular Reaction Dynamics and Chemical Reactivity* (Oxford, Oxford, 1987).

[9] (a) J. J. F. Ramaekers, H. K. van Dijk, J. Langelaar, and R. P. H. Rettschnick, Faraday Discuss. Chem. Soc. **75**, 183 (1983); (b) J. J. F. Ramaekers, L. B. Drignen, H. J. Lips, J. Langelaar, and R. P. H. Rettschnick, Laser Chem. **2**, 125 (1983); (c) M. Heppener, A. G. M. Kunst, D. Bebelaar, and R. P. H. Rettschnick, J. Chem. Phys. **83**, 5341 (1985); (d) M. Heppener and R. P. H. Rettschnick, in *Structure and Dynamics of Weakly Bound Molecular Complexes*, edited by A. Weber (Reidel, Dordrecht, 1987).

[10] E. R. Bernstein, K. Law, and M. Schauer, J. Chem. Phys. **80**, 634 (1984).

[11] G. E. Ewing, J. Phys. Chem. **90**, 1790 (1986); **91**, 4662 (1987).

[12] P. M. Weber and S. A. Rice, J. Phys. Chem. **92**, 5470 (1988).